



## MR angiography of the chest

Florian M. Vogt, MD\*, Mathias Goyen, MD, Jörg F. Debatin, MD, MBA

*Department of Diagnostic and Interventional Radiology, University Hospital Essen, Hufelandstrasse 55, 45122 Essen, Germany*

Within less than a decade following its initial description by Prince et al in 1993 [1], three-dimensional contrast-enhanced MR angiography (MRA) has been firmly established as an accurate noninvasive alternative for the diagnostic assessment of almost all vascular territories including the intrathoracic vessels. The technique combines the intravenous administration of paramagnetic contrast agents with the ultrafast acquisition of T1-weighted three-dimensional gradient echo data sets [1]. Contrast-enhanced three-dimensional MRA exploits the contrast-induced T1 shortening effects during the intra-arterial phase of the contrast agent. The availability of high-performance gradient systems permits the acquisition of complex three-dimensional data sets within the confines of a comfortable breathhold interval of under 30 seconds.

Contrast-enhanced three-dimensional MRA is able to overcome known limitations of conventional black blood and bright blood MRA techniques including cardiac and respiratory pulsation artifacts, poor signal-to-noise, susceptibility effects, and artifacts at air-tissue interfaces. Image quality is no longer related to flow or saturation [2,3]. Cardiac or respiratory gating is no longer necessary.

This article describes existing state-of-the-art contrast-enhanced three-dimensional MRA techniques for the assessment of the intrathoracic arterial and venous systems. Technique-related aspects are highlighted and the existing clinical experiences are summarized. Finally, developing techniques, which

are likely to enhance further the impact of thoracic MRA in the future, are discussed.

### Technical considerations

Contrast-enhanced three-dimensional MRA of the thoracic vasculature offers several advantages over conventional MRA techniques, including shorter acquisition times and high spatial resolution in conjunction with high signal- and contrast-to-noise. In many centers, the availability of contrast-enhanced three-dimensional MRA has profoundly impacted diagnostic strategies for exploring the thoracic vascular system [4–6]. Requiring only a peripheral intravenous catheter and administration of contrast agents characterized by an excellent safety profile [7,8], three-dimensional MRA techniques has vastly lowered the threshold for assessing the arterial and venous morphology of the thoracic vessels.

Paramagnetic contrast agents are pivotal for displaying the vascular system with fast three-dimensional gradient echo sequences. Without the presence of paramagnetic contrast, these sequences, characterized by very short repetition and echo times, render nondiagnostic images void of any intravascular signal. The presence of paramagnetic contrast in the vascular system over the length of the data acquisition period is crucial for successful contrast-enhanced three-dimensional MRA.

Paramagnetic contrast shortens the T1 relaxation time of blood. Gadolinium (Gd), the most commonly used paramagnetic substance, has a high relaxivity and a favorable safety profile when bound to a chelate. During the short intravascular phase the intravenously injected T1 shortening contrast agent provides signal in the arterial and venous systems,

---

\* Corresponding author.

*E-mail address:* florian.vogt@uni-essen.de (F.M. Vogt).

elevating the vessel to background contrast-to-noise ratio and eliminating flow artifacts. The signal of flowing blood is no longer flow-dependent. Flow-induced artifacts seen with noncontrast time-of-flight or phase-contrast MRA techniques are largely eliminated, and images can be collected in the plane coinciding with the course of the vessels of interest. This allows coronal coverage of large vascular territories in short imaging times and generates images that are similar in appearance to conventional catheter-based radiograph angiography [9].

Although similar in principle to spiral CT angiography, contrast-enhanced MRA holds considerable advantages. Beyond the absence of ionizing radiation and the ability to depict large vascular territories in three-dimensional imaging volumes, harmful side effects of the paramagnetic contrast agents used for the MRA examination are considerably less frequent and less severe than those associated with the iodinated contrast used in CT angiography. Paramagnetic contrast agents are nonnephrotoxic and have a low incidence of anaphylactoid reactions [8]. They are safe for use in patients with renal insufficiency and in patients with a history of allergic reactions to iodinated contrast media. Finally, on contrast-enhanced three-dimensional MRA images only the contrast-filled vessels are displayed. In addition, bones and calcium remain dark facilitating interpretation and subsequent postprocessing of the underlying three-dimensional data sets.

Contrast-enhanced three-dimensional MRA has been shown to be useful for the depiction of the supra-aortic arteries, the thoracic and abdominal aorta, and its major branch vessels. In its initial implementation, lengthy imaging times ranging between 3 and 5 minutes precluded data acquisition during a breathhold [10]. Ensuing respiratory motion artifacts considerably degraded image quality. Breathhold data acquisition did become possible with the use of improved gradient systems permitting considerable reductions in the minimum repetition (TR) and echo times (TE) [9,11]. The implementation of fast three-dimensional gradient echo sequences on high-performance systems permits the acquisition of complex three-dimensional data sets within the confines of a comfortable breathhold in as little as 5 to 20 seconds [12]. This dramatic reduction of scan time has even allowed the collection of temporally resolved three-dimensional data sets [13]. The transit of the paramagnetic contrast agent through the vascular system can be depicted. Ultrafast three-dimensional data acquisitions in conjunction with fast table feeds also permit chasing the contrast bolus through several vascular territories extending all the way to whole body MRA [14,15].

### *Paramagnetic contrast*

There are several paramagnetic contrast agents available today. Currently, only extracellular nonbinding Gd chelates with a concentration of 0.5 mol/L have regulatory approval for use in humans [16]. In the United States, no agent is currently approved for MRA by the Food and Drug Administration and any such use constitutes off-label use of an approved drug. Several paramagnetic intravascular Gd-based agents and superparamagnetic compounds are currently undergoing clinical and preclinical testing [17–20].

With higher infusion rates the local concentration of the contrast in the vessel of interest is higher, but because of a faster venous return there is a shorter arterial-venous time window for imaging. Contrast compounds with higher concentration formulations, such as Gadovist 1 mol/L (Schering, Berlin, Germany), might be advantageous when slow infusion protocols are used. Preliminary results comparing a 0.5 mol/L contrast agent (Magnevist, Schering, Berlin, Germany) with Gadovist 1 mol/L in pelvic MRA are very promising with regard to arterial enhancement [21].

Some newer agents, such as Multihance (Bracco, Milan, Italy), have higher relaxivity because of a transient binding to albumin and different routes of excretion but are still distributed into the extracellular space. Blood pool or intravascular contrast agents are sufficiently large or bind to large molecules when injected. This prevents them from leaking out of the capillaries and confines them to the intravascular compartment for extended periods of time. The major disadvantage of intravascular contrast agents is the early venous enhancement leaving a short window for arterial imaging. This represents a particular problem in the lower legs, where venous overlap can seriously impair the ability to assess the arteries. These agents are likely to play a dominant role in the assessment of the coronary arteries [22,23].

In view of the rapid progress of MRA techniques using extracellular agents, the future of intravascular contrast agents for morphologic imaging of the arterial vascular tree (with the exception of the coronary arteries) remains uncertain.

The paramagnetic agent is generally administered by an intravenous catheter placed into an antecubital vein. To achieve maximal image quality, the presence of the intravenously administered contrast bolus in the vascular territory under consideration must coincide with the data acquisition period. Several manual and automated techniques are available to ensure proper timing of the scan delay and are discussed later. Maximal contrast concentration in the vessel of

interest should be achieved during the acquisition of the central, contrast-determining portion of k-space.

Poor timing of the contrast application affects image quality in different ways: venous overlap, ringing artifacts, or insufficient signal within the vessels of interest can occur [24,25]. To ensure the exact synchronization of arterial enhancement with the acquisition of arterial-phase Gd-enhanced three-dimensional MRA, different strategies have been developed to optimize timing including the use of a test bolus, fluoroscopic triggering, and an automated detection system, which triggers the initiation of scanning when contrast material is detected in a predefined area of interest. Optimal timing of contrast administration results in three-dimensional MRA data sets void of ringing artifacts and venous overlap [26].

Using a fixed scan delay is the simplest means of applying the paramagnetic contrast agent and works in most instances for MRA of the thoracic arteries [27]. The contrast bolus should commence 10 seconds before the beginning of data acquisition and encompass the entire scan time. Age, body weight, and heart rate are some of the parameters that make it more difficult to predict the circulation time. Test bolus timing techniques are established and simple to use. Following the injection of a 1- to 2-mL test bolus of paramagnetic contrast, images of the target vessel are collected using a rapid two-dimensional gradient-echo pulse sequence, preferably in the axial plane, with a temporal resolution of one image every 1 to 2 seconds. Arrival of contrast agent is detected by a transient signal increase, hence the appropriate time delay to align the central k-space with arterial enhancement can be calculated [9,28]. For centrically encoded sequences, the delay of data acquisition corresponds to the time the test bolus needs to reach the target volume. Recent investigations reveal that examinations after bolus testing showed significantly superior signal-to-noise ratio (SNR) as compared with examinations without a test bolus [29].

Other bolus-timing techniques are based on real-time triggering. There are two similar approaches. Line scanning measures the signal intensity within an operator-defined monitoring volume and subsequently initiates data acquisition following bolus arrival automatically [30]. Hand fluoroscopic imaging uses visual cues identifying the contrast agent to be present in the vessels under investigation. The three-dimensional MRA sequence is subsequently triggered manually to capture peak contrast. These timing methods generally are based on the use of centric view ordering of k-space for the three-dimensional acquisition. The fluoroscopic-triggered three-

dimensional elliptical centric view ordering technique has shown a reliability exceeding 90% in detecting the bolus arrival [31,32].

Faster gradient sets now permit for the acquisition of time-resolved three-dimensional MRA. To enhance the speed of data collection further these techniques use a host of methods including variable-rate k-space sampling, view sharing, temporal interpolation, and zero filling. The method ensures the acquisition of data and reconstruction of images at time points before, during, and after the contrast agent passes through the vessels of interest. The need for timing the contrast bolus is eliminated [13,33,34]. Time-resolved three-dimensional MRA is highly robust because it is virtually operator independent. In most applications the required high temporal resolution can be achieved only at the price of compromising spatial resolution. The application of sensitivity encoding and simultaneous magnetization of spatial harmonics parallel imaging techniques is likely to provide both high temporal and spatial resolution [35].

Intravenously administered Gd doses range between 0.05 and 0.3 mmol/kg body weight depending on the vascular territory under investigation. Doses between 0.1 and 0.2 mmol/kg body weight Gd-based contrast agent were reported to be sufficient for most single-station MRA examinations [7,16]. Even lower dosing (0.075 mmol/kg) can be used in time-resolved MRA [36]. The resulting injection volume of 15 to 40 mL should be administered at a rate between 1.5 and 2.5 mL/second. The role of injection rate on image quality is still being determined. If the injection rate is too fast, k-space modulation occurs, degrading image quality and increasing ringing artifacts [25]. Carroll et al [24] determined that lowering the injection rate reduces changes in signal versus time and results in less blurring without a significant loss of vessel contrast.

The actual flow rate should be adjusted to ensure injection of the entire contrast volume in a period not exceeding the acquisition time. Regardless of the timing regimen or imaging technique, use of an automated injector facilitates contrast timing and delivery because it allows precise infusion using predefined weight-adjusted rates and volumes.

For imaging the thoracic veins, diluted contrast (1:10 to 20) should be injected directly into the affected side. For a comprehensive display of the entire venous system, both arms can be injected simultaneously. An alternative method for central venous imaging is to administer a diluted dose of Gd-chelate contrast media directly into the vein of interest [37,38].

### Pulse sequence considerations

The pulse sequence design for contrast-enhanced MRA is based on a three-dimensional Fourier transform gradient recalled echo (GRE) sequence using rapid radiofrequency pulsing. Optimization of MRA is related to rapid data collection. The fastest possible three-dimensional imaging sequence, typically a fast three-dimensional gradient echo pulse, should be used. To achieve maximal T1 weighting, spoiled sequences should be used. Spoiling is useful because it destroys the residual magnetization after each echo and magnifies the effect of T1 relaxation agents. Repetition and echo times should be as short as possible. The newest generation of commercially available 1.5-T MR imaging scanners provides three-dimensional gradient echo pulse sequences with minimal repetition times of less than 2 milliseconds and minimal echo times of less than 1 millisecond. A flip angle ranging between 10 and 25 degrees provides adequate suppression of the surrounding tissues and has been shown to render excellent image quality: the longer the repetition time, the lower the flip angle.

Thoracic contrast-enhanced three-dimensional MRA data need to be collected within a breathhold to minimize the artifacts related to respiratory motion. The partition dimensions (ie, partition thickness, matrix size, and field-of-view) should be prescribed to achieve the smallest possible voxel size to allow for sufficient spatial coverage of the target vessel. Section thickness should be adjusted to be between

1.5 and 2.5 mm to ensure full coverage of the vascular system under consideration and still permit multiplanar reformations. To ensure full coverage, between 48 and 64 thin contiguous sections need to be collected.

Imaging time can be decreased further using partial Fourier imaging, decreased number of partitions, decreased phase-encoding steps, or a rectangular field of view. Widening bandwidth also makes for faster scanning, although this causes a reduction in SNR. These improvements in image speed can be used to improve image resolution (ie, decrease voxel size). Zero-filling, although not improving the true spatial resolution, generates better reformations and maximum intensity projections and reduces partial volume averaging errors. Sensitivity encoding and simultaneous magnetization of spatial harmonics imaging are newly developed techniques that enable further reductions in scan time, while maintaining spatial resolution (Fig. 1). The accompanying 30% to 55% reduction in SNR does not seem to affect image quality adversely because of the high concentration of the contrast compound in the vasculature during data collection [39,40].

It is well recognized that, to ensure image quality, the contrast must be near or at the peak concentration in the vasculature of interest when acquiring the central phase-encoding views of the MRA. In principle there are two different methods for k-space phase ordering: conventional sequential phase ordering where the center k-space views are collected in

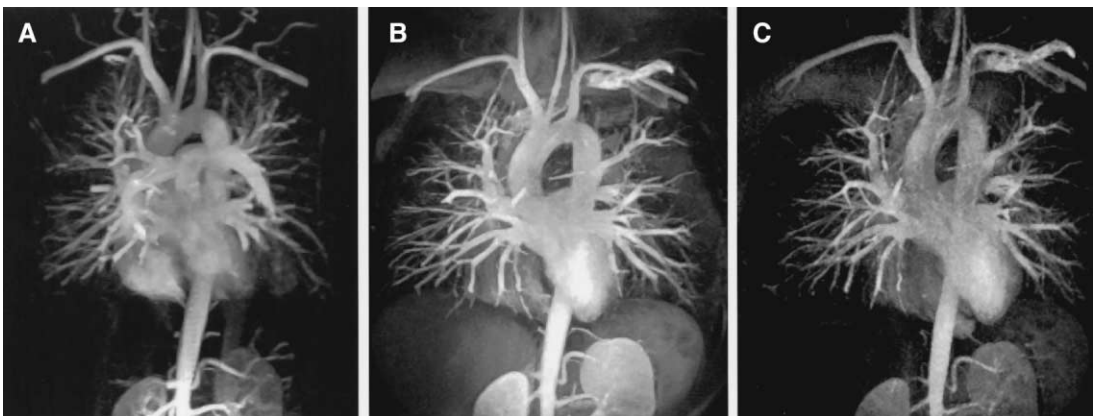


Fig. 1. Normal contrast-enhanced MRA of the thoracic aorta in a 28-year-old healthy volunteer acquired in the coronal plane. (A) Maximum intensity projection (MIP) reformation of a coronal three-dimensional MRA data set using a standard phased array coil. (B) Coronal MIP image achieved with twofold simultaneous magnetization of spatial harmonics reduction using a new six-element cardiac array. (C) Coronal MIP image with twofold sensitivity encoding reduction. A spatial resolution of  $1.7 \times 0.8 \times 1.8 \text{ mm}^3$  was achieved with decrease of scan time almost to 50% in Fig. 1B and C. Despite the intrinsic drawback in signal-to-noise ratio, the coronal MIP is of nearly identical diagnostic value.

the middle of the imaging period, and centric phase ordering that enables the acquisition of the crucial image contrast data at the beginning of the sequence [9]. View order with elliptic centric phase encoding has been shown to be centric in both phase-encoding directions, which provides minimal sensitivity to motion artifact caused by loss of breathhold [32,41]. To facilitate the timing of the contrast bolus most manufacturers now provide centrally encoded sequences for the performance of MRA.

### Other techniques

The recently developed steady-state free precession (SSFP) gradient echo sequence (ie, TrueFISP, FIESTA, balanced fast field echo) is characterized by balanced gradients in all three directions, ensuring maximum recovery of the transverse magnetization [42,43]. At the end of the TR, the transverse magnetization is refocused, and the next excitation can be started without further preparation. The image contrast with SSFP is determined by favorable T2\*-T1 properties that are nearly independent from blood flow [44]. The main advantage of this sequence

relates to its high signal of fluids, which results in high contrast delineating vessels as bright structures, while at the same time delineating all other morphology. The use of short TRs is mandatory to avoid T2\* effects and can only be achieved using the most powerful gradient systems. The short TR and echo time reduce susceptibility artifacts and lead to extremely short data acquisition times. Reductions in acquisition time by a factor of two or three can be achieved at similar temporal and spatial resolution in comparison with conventional segmented k-space gradient echo imaging. Other potential applications could be the real-time assessment of intimal flap movement in aortic dissection delineating the relationship to branch vessels and possible occlusion of these during systolic or diastolic phase. In addition, differentiation between true and false lumen or possible thrombus and slow-flowing blood can be done easily (Fig. 2).

A vulnerable point in SSFP is patient-induced B<sub>0</sub> inhomogeneities. A local shim volume should be used to eliminate these effects locally. Although there is increasing interest assessing global and regional ventricular dimensions and cardiac functions, SSFP has not been proved as the modality of choice for

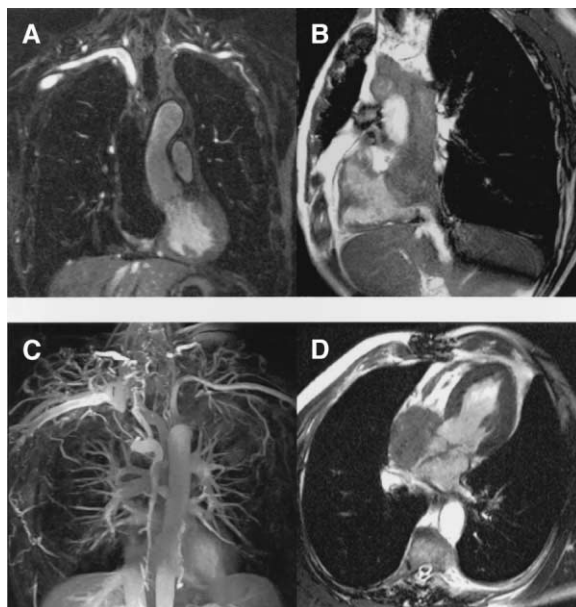


Fig. 2. A 57-year-old man with unknown right-sided chest pain and raised central venous pressure. Exclusion of suspected central, chest tumor. (A) Coronal view of venous three-dimensional MRA data set delineating lack of contrast filling in the vena cava superior. (B) Sagittal view of cine-mode TrueFISP sequence allowing differentiation between completely obstructed vena cava superior and partially thrombosed right atrium and slow-flowing blood. (C) Coronal maximum intensity projection of the thoracic vessels in venous phase missing the vena cava superior and delineating collateral flow in azygos and cervicothoracic veins. (D) TrueFISP four-chamber view showing almost complete clotting of right atrium.

MRA because, until now, cine MR imaging has relied exclusively on single-slice techniques requiring multiple breathhold [44–46]. For instance, coverage of the entire aorta required scan times of more than 10 minutes and variations in inspiratory depth led to discontinuous coverage of the data sets. Recently developed multislice real-time SSFP cine sequences capable of covering the entire thoracic or abdominal aorta in the axial plane promises to resolve these problems. For this technique, ECG triggering is needed to synchronize the slices [47].

Another, more troublesome limitation of SSFP is its enhancement of fat in addition to fluids. This hinders the postprocessing of maximum intensity projections. Because of the impact this has on image evaluation, the usefulness of real-time cine SSFP in vessel imaging remains doubtful.

### Image analysis

The high contrast between Gd-containing luminal (bright) and extraluminal (dark) spins and the true three-dimensional nature of the acquired data sets provides the basis for using a variety of postprocessing algorithms. Analysis should never be limited to maximum intensity projections or surface-shaded display. The three-dimensionality inherent to the technique can only be exploited fully if the data are viewed interactively on a workstation using multiplanar reformations. Endoluminal, virtual angioscopic images can also be obtained, but their clinical relevance is very limited.

### Clinical applications

Contrast-enhanced three-dimensional MRA has proved to be a versatile noninvasive imaging modality for analysis of thoracic arteries and veins. In the following sections various imaging indications involving the thoracic aorta, the pulmonary arteries and pulmonary veins, and the thoracic systemic veins are discussed.

#### *Thoracic aorta*

Although CT remains the modality of choice in all acute, life-threatening conditions involving the thoracic aorta, contrast-enhanced three-dimensional MRA has emerged as the imaging modality of choice for assessing the thoracic aorta in the more stable patient. The technique overcomes respiratory and cardiac motion artifacts, which impair noncontrast

MRA image quality to the point of rendering scans of the thoracic aorta nondiagnostic. The underlying three-dimensional GRE sequences permit data acquisition of large fields-of-view in apnea and do not require cardiac gating. Pulsatility artifacts, however, sometimes make it difficult to assess the supra-valvular portion of the ascending thoracic aorta.

#### *Aortic dissection*

Beyond establishing the presence of dissection, it is crucial to define the localization and extent of disease. In fact, the location and relationship of the intimal tear are critical to the choice of subsequent therapeutic management. The Stanford classification separates aortic dissections affecting the ascending aorta (Stanford A) from those merely affecting the descending aorta (Stanford B). Type A dissections harbor the risk of myocardial infarction because of an extension of the dissection into the coronary arteries and of pericardial tamponade secondary to aortic rupture into the pericardium. Type A dissections require emergent surgery. Dissections arising distal to the left subclavian (Stanford B) are less precarious and are usually managed medically.

The efficacy of three-dimensional MRA in the assessment and follow-up of aortic dissection is well established. Three-dimensional MRA of the thoracic aorta is fast and combines the advantages of arterial contrast, similar to conventional catheter angiography, with cross-sectional information. Using multiplanar reformations, three-dimensional MRA provides a comprehensive analysis in suspected aortic dissection: the extent and relationship to branch vessels can be depicted fully, and the true lumen can be separated from the false lumen (Fig. 3).

The three-dimensional data set should be obtained in the orientation optimal for visualization of the target structure. The diagnostic value of three-dimensional contrast MRA is limited to the assessment of the aortic lumen. Because aortic dissection can occur without an intimal flap (intramural hematoma) or inflammatory diseases (aortitis), an additional delayed T1-weighted sequence, collected following contrast administration, is recommended. For this purpose, the three-dimensional contrast MRA sequence can be repeated 2 minutes following the contrast administration or alternatively a T1-weighted GRE or spin echo sequence can be acquired in the axial plane. Although ECG gating is not necessary for the collection of a three-dimensional data set, T1-weighted GRE or spin echo sequences need to be used in conjunction with ECG gating. On T1-weighted spin echo images, the intramural hematoma is identified as concentric thickening of the aortic wall with increased intramural

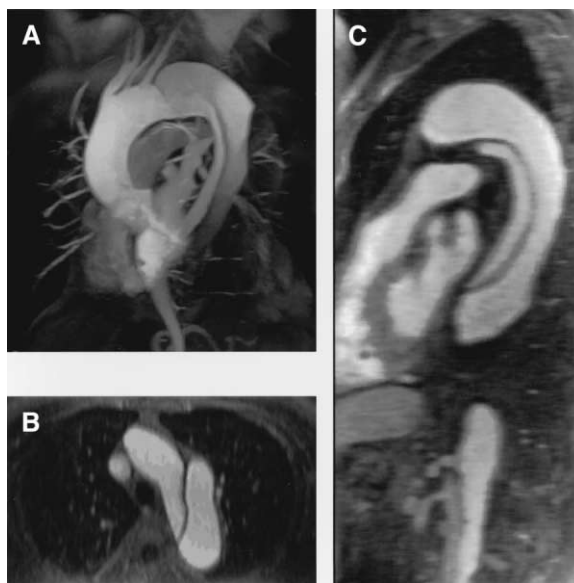


Fig. 3. A 64-year-old man with acute thoracic pain. (A) Maximum intensity projection reformats of coronal three-dimensional MRA data set (oblique sagittal plane) demonstrate aortic dissection distal to the origin of the left subclavian artery. (B) Axial multiplanar reformation. (C) Sagittal multiplanar reformation.

signal intensity. Inflammatory processes also show enhancement of the aortic wall and surrounding soft tissues [10].

Additional functional information can be gathered with the use of cine imaging. Cine phase contrast acquisitions permit measurement of flow velocities and flow volumes and can easily differentiate between true and false lumen. Even aortic valve involvement caused by dissection can be evaluated. The severity of valvular regurgitation can be determined with cine gradient echo MR imaging, which allows measurement of the area of the signal void corresponding to the abnormal flow jet. Alternatively, this modality can be used to obtain ventricular volumetric measurements and calculate the regurgitant fraction or velocity-encoded cine. MR imaging can be used to quantify regurgitant blood flow [48].

#### *Aortic aneurysm*

Thoracic aortic aneurysms may be classified according to their location, etiology, or shape. Natural history studies of thoracic aortic aneurysms report a 1- and 5-year survival of 39% to 52% and 13% to 19%, respectively [49]. Most mortality in patients with thoracic aortic aneurysms is related to aneurysm rupture. Thoracic aortic aneurysm is a highly lethal condition warranting consideration of elective, prophylactic surgical repair. The timing of

surgery is often a difficult clinical decision, however, particularly in asymptomatic patients or those with comorbid conditions.

A recommendation of surgery represents a balance. Clinicians must weigh estimates of thoracic aortic aneurysm natural history and rupture risk against operative mortality and complication rate. This risk is related to the site, etiology, size, and expansion rate of the aneurysm. MR imaging of an aortic aneurysm can demonstrate the site of aneurysm, its length, morphology, and relationship of the aneurysm to branch vessels and the presence of mural thrombus or a penetrating ulcer. All of these findings can affect surgical decision making. Furthermore, the aortic valve needs to be assessed for the presence of valvular stenosis or insufficiency.

Complex underlying arterial morphology in patients with thoracic aortic aneurysm may result in an inadvertent exclusion of important portions of the arterial anatomy from the three-dimensional imaging volume. It is important to conduct the localizing process carefully using breathhold techniques (Fig. 4). For imaging aortic aneurysms, which contain slow flow, it is important to anticipate a long contrast travel time to fill the entire aorta. As mentioned previously, three-dimensional MRA contains little information about the morphology of the aortic wall, and should be complemented by T1-weighted post-contrast images in diagnosis of an aneurysm.

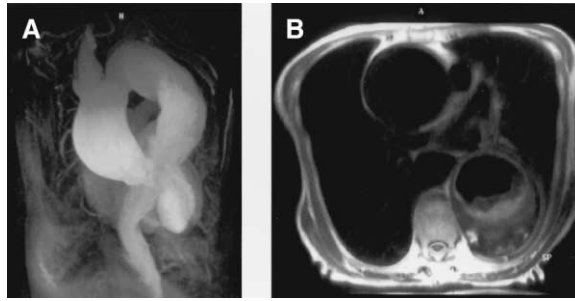


Fig. 4. Excessive aneurysm of the ascending aorta. (A) Sagittal maximum intensity projection projection demonstrates the aneurysm originating immediately above the aortic valve and involving the supra-aortic vessels. (B) Axial half-Fourier single-shot turbo spin echo sequence delineating an extensive wall-adherent thrombus in the posterior part of descending aorta. No dissection was observed.

Stenosis or occlusion of the great vessels may be caused by atherosclerosis, dissection, and arteritis. Other rare causes include fibromuscular dysplasia, postradiation arteritis, and mediastinal inflammatory or neoplastic disease. The patient commonly presents with upper extremity ischemia or neurologic symptoms from the steal phenomena during arm exercise. Coronal three-dimensional Gd-MRA is the best sequence to assess origins of the innominate artery, common carotids, vertebral, and subclavian arteries.

#### *Developmental abnormalities*

MR imaging can safely assess less common congenital cardiovascular malformations of the aorta, including arch anomalies and aortic coarctation. Coarctation may be described as preductal, juxtaductal, or postductal. The more common juxtaductal or

postductal types occur as a discrete focal narrowing of the aortic isthmus distal to the origin of the left subclavian artery and near the aortic end of the ductus arteriosus (Fig. 5). Depending on the severity of the coarctation and obliteration of ductus arteriosus, an abundance of collateral vessels may be seen. MR imaging and MR imaging velocity mapping have proved to visualize the anatomy and severity of the coarctation accurately [50]. Gd-enhanced three-dimensional MRA has the advantage for image reconstructions in any desirable orientation providing an accurate overview especially useful in tortuous vessel structures. An apparent coarctation may be recognized as a pseudocoarctation. The rapid acquisition time enables successful contrast-enhanced MRA in children including neonates and infants [51]. Quantitative measurements can be obtained by using velocity-encoded cine MRA [52].

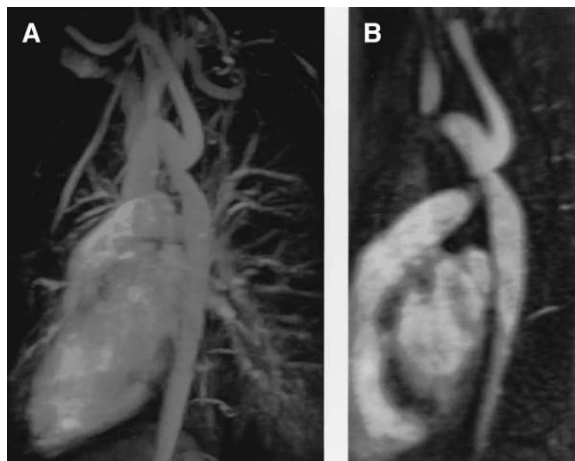


Fig. 5. A 28-year-old man with coarctation of the aorta. Note the dilated proximal left subclavian artery. (A) Sagittal maximum intensity projection projection. (B) Corresponding sagittal multiplanar reformation.

### Central thoracic veins

Thrombosis of systemic chest veins is an important cause of morbidity in patients with malignancy, hematologic disease, or long-term indwelling catheters. Prompt diagnosis and adequate therapy need to be provided to restore patency of the veins.

Thrombo-occlusive disease of the chest veins has been evaluated accurately by MR imaging using two-dimensional time-of-flight methods [53,54]. These techniques have the advantage of not requiring contrast material but are limited by long examination times and potentially misleading artifacts [53,55]. Recent reports have proposed the use of Gd-enhanced three-dimensional MR venography techniques [56]. With the advent of high-performance gradient systems, data collection times have been reduced to acquire a three-dimensional data set within a breathholding after the intravenous injection of contrast agent.

In general, two approaches are pursued. Initially, direct MR venography is performed using an injection of diluted contrast media to avoid T2 shortening effects bolus. In comparison with two-dimensional time-of-flight techniques, several recently published studies show better image quality within shorter imaging times when evaluating deep venous thrombosis [38]. Thornton et al [57] obtained breathholding three-dimensional spoiled GRE during first pass and in the delayed arteriovenous phase after manual intravenous Gd bolus injection resulting in 100% sensitivity and specificity. First-pass imaging, however, requires venous access site in the clinically symptomatic limb and does not allow for a complete evaluation of the chest veins, even with bilateral infusion [58].

With an indirect approach, the veins are imaged during the contrast equilibrium phase following the injection of paramagnetic contrast into an antecubital

vein. To compensate for considerable dilution as the contrast passes through the lungs, the arterial system, and the capillary bed, indirect MR venography requires large doses of contrast. The indirect approach does not require cannulation of the vein in the effected extremity. For better contrast-to-noise, images obtained in the venous phase can be subtracted from those acquired in the arterial phase [59]. The timing of the acquisition relative to the contrast administration is crucial. Kroenke et al [58] extrapolated the mean time of maximum contrast enhancement of the thoracic veins and chose a time delay of 15 seconds between the acquisition of the arterial and venous phase. The introduction of dynamic Gd-enhanced three-dimensional MR venography, based on the use of very short TR (1.6 millisecond) and TE (0.6 millisecond) [60] permits the acquisition of six three-dimensional data sets in under 24 seconds. This method obviates the need for contrast bolus timing and has been shown to be reliable for the display of central veins. This type of dynamic imaging also allows for the assessment of thoracic veins in different arm positions (Fig. 6).

Another MR venography approach using a high-resolution TrueFISP imaging sequence promises visualization of thrombus with high contrast relative to the surrounding blood pool without requiring the administration of contrast agents. Limited investigations of patients with deep vein thrombosis have been promising [61].

### Pulmonary arteries

MR imaging of pulmonary vasculature has been challenging for a variety of reasons. Particularly, respiratory motion and poor contrast between flowing blood and emboli have contributed toward poor results [62]. Faster gradient hardware combined with the dynamic administration of paramagnetic contrast

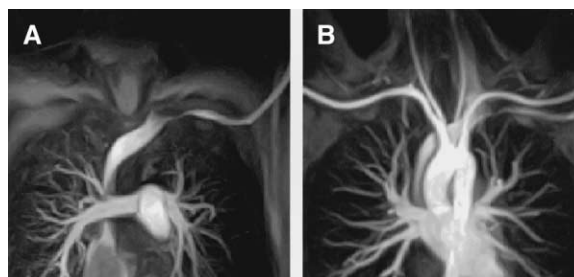


Fig. 6. A 29-year-old male conductor with left-sided arm weakness and known occlusion of subclavian and internal jugular vein of the right side. Left-sided functional subclavian vein stenosis at the transition to brachiocephalic vein was suspected and proofed using dynamic three-dimensional MRA. (A) Coronal maximum intensity projection (MIP), early phase. (B) Coronal MIP, late phase.



Fig. 7. A 47-year-old woman with left pleuritic chest pain. Coronal maximum intensity projection of a time-resolved contrast-enhanced three-dimensional MRA data set of the pulmonary arteries shows an embolus in the distal left artery (*arrow*).

permits display of the pulmonary vasculature. Two MR imaging-based approaches to assess the pulmonary arteries have been suggested: a sagittal acquisition strategy using two separate examinations requiring twice the contrast volume versus the acquisition of a single coronal three-dimensional volume set encompassing both lungs [63–66]. The advantage of sagittal imaging lies in the reduced

imaging volume, which permits shortening of the data acquisition time. The coronal acquisition approach exploits a single large field of view that encompasses both lungs and has the advantage of visualizing both central and peripheral pulmonary vasculature (Fig. 7). Reflecting ease of interpretation most investigators today would use the coronal data acquisition technique.

By reducing TR to less than 2 milliseconds and TE to less than 1 millisecond, temporally resolved three-dimensional MRA becomes possible. The acquisition time of the entire pulmonary tree can be reduced to less than 4 seconds using the latest hardware and software for the collection of a single coronal three-dimensional data set [33]. Even in patients with respiratory distress and limited breath-holding capabilities the data collection time is sufficiently short to permit artifact-free depiction of the pulmonary arterial tree. Although spatial resolution has remained limited in most implementations, contrast-enhanced three-dimensional MRA was shown to be capable of detecting subsegmental emboli.

A major advantage of MRA over alternative diagnostic strategies for investigation of patients with suspected thromboembolic disease relates to the fact that MRA of the pulmonary vasculature can be complemented by MR venography of the pelvic and femoral veins. Vascular anomalies including arteriovenous malformations, anomalous pulmonary veins and pulmonary sequestration, patent ductus arteriosus, or pulmonary atresia associated with congenital heart disease can also be detected (Fig. 8) [67]. Pulmonary hypertension documented by three-dimensional MRA provides a better delineation of the central pulmonary arteries than conventional angiography, where the catheter may be advanced into the pulmonary arteries beyond significant pathologies.

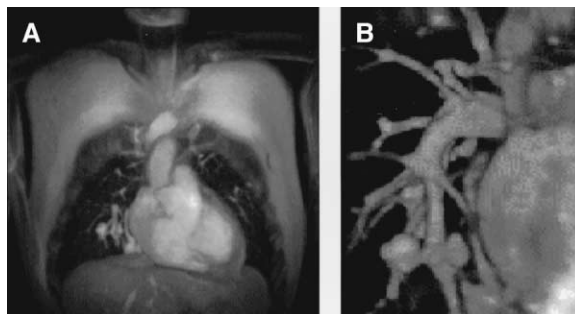


Fig. 8. A 49-year-old man with suspected pulmonary arteriovenous malformation on chest radiograph in the right lower lobe. The three-dimensional MRA data set revealed the feeding vessels and sharp delineated small nodules. The diagnosis was Osler-Weber-Rendu disease. (A) Coronal maximum intensity projection reconstruction. (B) Shaded surface reconstruction anteroposterior view of the arteriovenous malformation.

Illustration of the pulmonary veins is also provided by contrast-enhanced three-dimensional MRA. Venous structures are seen if the central k-space lines are obtained during the venous or equilibrium phase of the contrast bolus. The timing of the central k-space views relative to contrast administration is crucial. The need for timing can be overcome by collecting multiple three-dimensional data sets in various vascular phases using sequential three-dimensional imaging with ultrafast three-dimensional sequences. For the optimal display of the pulmonary veins, a data set containing both pulmonary veins and arteries is subtracted from a solely arterial data set [68]. Better separation of arteries and veins can be achieved using higher infusion rates and lower contrast media doses in multiphase MR imaging protocols. Visualization of main pulmonary veins, segmental veins, and subsegmental veins up to the fourth order can be achieved.

## Summary

Using the described strategies all relevant disease processes of the thoracic vessels can be fully depicted using contrast-enhanced three-dimensional MRA. The aorta and the major neck and arm vessels are well visualized. Vascular pathologies, such as aneurysms, dissections, and occlusions, are readily recognized. With the implementation of high-performance gradients, three-dimensional MRA of the pulmonary vasculature has become possible even in dyspneic patients. Congenital lesions, such as coarctations, are particularly well suited for analysis with these techniques.

## References

- [1] Prince MR, Yucel EK, Kaufman JA, et al. Dynamic gadolinium-enhanced three-dimensional abdominal MR arteriography. *J Magn Reson Imaging* 1993; 3:877–81.
- [2] Leung DA, McKinnon GC, Davis CP, et al. Breath-hold, contrast-enhanced, three-dimensional MR angiography. *Radiology* 1996;200:569–71.
- [3] Prince MR, Narasimham DL, Stanley JC, et al. Breath-hold gadolinium-enhanced MR angiography of the abdominal aorta and its major branches. *Radiology* 1995;197:785–92.
- [4] Hartnell GG, Finn JP, Zenni M, et al. MR imaging of the thoracic aorta: comparison of spin-echo, angiographic, and breathhold techniques. *Radiology* 1994; 191:697–704.
- [5] Krinsky GA, Rofsky NM, DeCorato DR, et al. Thoracic aorta: comparison of gadolinium-enhanced three-dimensional MR angiography with conventional MR imaging. *Radiology* 1997;202:183–93.
- [6] Leung DA, Debatin JF. Three-dimensional contrast-enhanced magnetic resonance angiography of the thoracic vasculature. *Eur Radiol* 1997;7:981–9.
- [7] Goyen M, Ruehm SG, Debatin JF. MR-angiography: the role of contrast agents. *Eur J Radiol* 2000;34: 247–56.
- [8] Shellock FG, Kanal E. Safety of magnetic resonance imaging contrast agents. *J Magn Reson Imaging* 1999;10:477–84.
- [9] Hany TF, McKinnon GC, Leung DA, et al. Optimization of contrast timing for breathhold three-dimensional MR angiography. *J Magn Reson Imaging* 1997; 7:551–6.
- [10] Prince MR. Gadolinium-enhanced MR aortography. *Radiology* 1994;191:155–64.
- [11] Prince MR, Chenevert TL, Foo TK, et al. Contrast-enhanced abdominal MR angiography: optimization of imaging delay time by automating the detection of contrast material arrival in the aorta. *Radiology* 1997; 203:109–14.
- [12] Prince MR. Contrast-enhanced MR angiography: theory and optimization. *Magn Reson Imaging Clin N Am* 1998;6:257–67.
- [13] Korosec FR, Frayne R, Grist TM, Mistretta CA. Time-resolved contrast-enhanced 3D MR angiography. *Magn Reson Med* 1996;36:345–51.
- [14] Goyen M, Quick HH, Debatin JF, et al. Whole-body three-dimensional MR angiography with a rolling table platform: initial clinical experience. *Radiology* 2002; 22:270–7.
- [15] Meaney JF, Ridgway JP, Chakraverty S, et al. Stepping-table gadolinium-enhanced digital subtraction MR angiography of the aorta and lower extremity arteries: preliminary experience. *Radiology* 1999; 211: 59–67.
- [16] Hany TF, Schmidt M, Hilfiker PR, et al. Optimization of contrast dosage for gadolinium-enhanced 3D MRA of the pulmonary and renal arteries. *Magn Reson Imaging* 1998;16:901–6.
- [17] Earls JP, Bluemke DA. New MR imaging contrast agents. *Magn Reson Imaging Clin N Am* 1999;7: 255–73.
- [18] Knopp MV, von Tengg-Kobligk H, Floemer F, Schoenberg SO. Contrast agents for MRA: future directions. *J Magn Reson Imaging* 1999;10:314–6.
- [19] Lahti KM, Lauffer RB, Chan T, Weisskoff RM. Magnetic resonance angiography at 0.3 T using MS-325. *Magma* 2001;12:88–91.
- [20] Taupitz M, Schnorr J, Wagner S, et al. Coronary MR angiography: experimental results with a monomer-stabilized blood pool contrast medium. *Radiology* 2002;222:120–6.
- [21] Goyen M, Lauenstein TC, Herborn CU, et al. 0.5 mol/L Gd chelate (Magnevist) versus 1.0 mol/L Gd chelate (Gadovist): dose-independent effect on image quality of pelvic three-dimensional MR-angiography. *J Magn Reson Imaging* 2001;14:602–7.

- [22] Li D, Zheng J, Bae KT, et al. Contrast-enhanced magnetic resonance imaging of the coronary arteries: a review. *Invest Radiol* 1998;33:578–86.
- [23] Zheng J, Li D, Cavagna FM, et al. Contrast-enhanced coronary MR angiography: relationship between coronary artery delineation and blood T1. *J Magn Reson Imaging* 2001;14:348–54.
- [24] Carroll TJ, Korosec FR, Swan JS, et al. The effect of injection rate on time-resolved contrast-enhanced peripheral MRA. *J Magn Reson Imaging* 2001;14:401–10.
- [25] Svensson J, Petersson JS, Stahlberg F, et al. Image artifacts due to a time-varying contrast medium concentration in 3D contrast-enhanced MRA. *J Magn Reson Imaging* 1999;10:919–28.
- [26] Lee VS, Martin DJ, Krinsky GA, Rofsky NM. Gadolinium-enhanced MR angiography: artifacts and pitfalls. *AJR Am J Roentgenol* 2000;175:197–205.
- [27] Prince MR, Narasimham DL, Jacoby WT, et al. Three-dimensional gadolinium-enhanced MR angiography of the thoracic aorta. *AJR Am J Roentgenol* 1996;166:1387–97.
- [28] Earls JP, Rofsky NM, DeCorato DR, et al. Breath-hold single-dose gadolinium-enhanced three-dimensional MR aortography: usefulness of a timing examination and MR power injector. *Radiology* 1996;201:705–10.
- [29] Kreitner KF, Kunz RP, Kalden P, et al. Contrast-enhanced three-dimensional MR angiography of the thoracic aorta: experiences after 118 examinations with a standard dose contrast administration and different injection protocols. *Eur Radiol* 2001;11:1355–63.
- [30] Foo TK, Saranathan M, Prince MR, Chenevert TL. Automated detection of bolus arrival and initiation of data acquisition in fast, three-dimensional, gadolinium-enhanced MR angiography. *Radiology* 1997;203:275–80.
- [31] Fellner FA, Fellner C, Wutke R, et al. Fluoroscopically triggered contrast-enhanced 3D MR DSA and 3D time-of-flight turbo MRA of the carotid arteries: first clinical experiences in correlation with ultrasound, x-ray angiography, and endarterectomy findings. *Magn Reson Imaging* 2000;18:575–85.
- [32] Wilman AH, Riederer SJ, King BF, et al. Fluoroscopically triggered contrast-enhanced three-dimensional MR angiography with elliptical centric view order: application to the renal arteries. *Radiology* 1997;205:137–46.
- [33] Goyen M, Laub G, Ladd ME, et al. Dynamic 3D MR angiography of the pulmonary arteries in under four seconds. *J Magn Reson Imaging* 2001;13:372–7.
- [34] Hennig J, Scheffler K, Laubenberger J, Strecker R. Time-resolved projection angiography after bolus injection of contrast agent. *Magn Reson Med* 1997;37:341–5.
- [35] Sodickson DK, McKenzie CA, Ohliger MA, et al. Recent advances in image reconstruction, coil sensitivity calibration, and coil array design for SMASH and generalized parallel MRI. *MAGMA* 2002;13:158–63.
- [36] Frayne R, Grist TM, Swan JS, et al. 3D MR DSA: effects of injection protocol and image masking. *J Magn Reson Imaging* 2000;12:476–87.
- [37] Neimatallah MA, Ho VB, Dong Q, et al. Gadolinium-enhanced 3D magnetic resonance angiography of the thoracic vessels. *J Magn Reson Imaging* 1999;10:758–70.
- [38] Ruehm SG, Zimny K, Debatin JF. Direct contrast-enhanced 3D MR venography. *Eur Radiol* 2001;11:102–12.
- [39] Sodickson DK, McKenzie CA, Li W, et al. Contrast-enhanced 3D MR angiography with simultaneous acquisition of spatial harmonics: a pilot study. *Radiology* 2000;217:284–9.
- [40] Weiger M, Pruessmann KP, Leussler C, et al. Specific coil design for SENSE: a six-element cardiac array. *Magn Reson Med* 2001;45:495–504.
- [41] Naganawa S, Koshikawa T, Fukatsu H, et al. Contrast-enhanced MR angiography of the carotid artery using 3D time-resolved imaging of contrast kinetics: comparison with real-time fluoroscopic triggered 3D-elliptical centric view ordering. *Radiat Med* 2001;19:185–92.
- [42] Haacke EM, Tkach JA. Fast MR imaging: techniques and clinical applications. *AJR Am J Roentgenol* 1990;155:951–64.
- [43] Barkhausen J, Ruehm SG, Goyen M, et al. MR evaluation of ventricular function: true fast imaging with steady-state precession versus fast low-angle shot cine MR imaging: feasibility study. *Radiology* 2001;219:264–9.
- [44] Plein S, Bloomer TN, Ridgway JP, et al. Steady-state free precession magnetic resonance imaging of the heart: comparison with segmented k-space gradient-echo imaging. *J Magn Reson Imaging* 2001;14:230–6.
- [45] Thiele H, Nagel E, Paetsch I, et al. Functional cardiac MR imaging with steady-state free precession (SSFP) significantly improves endocardial border delineation without contrast agents. *J Magn Reson Imaging* 2001;14:362–7.
- [46] Bloomer TN, Plein S, Radjenovic A, et al. Cine MRI using steady state free precession in the radial long axis orientation is a fast accurate method for obtaining volumetric data of the left ventricle. *J Magn Reson Imaging* 2001;14:685–92.
- [47] Barkhausen J, Goyen M, Ruhm SG, et al. Assessment of ventricular function with single breathhold real-time steady-state free precession cine MR imaging. *AJR Am J Roentgenol* 2002;178:731–5.
- [48] Didier D, Ratib O, Lerch R, Friedli B. Detection and quantification of valvular heart disease with dynamic cardiac MR imaging. *Radiographics* 2000;20:1279–301.
- [49] Pitt MP, Bonser RS. The natural history of thoracic aortic aneurysm disease: an overview. *J Card Surg* 1997;12(suppl 2):270–8.
- [50] Holmqvist C, Stahlberg F, Hansens K, et al. Collateral flow in coarctation of the aorta with magnetic resonance velocity mapping: correlation to morphological

- imaging of collateral vessels. *J Magn Reson Imaging* 2002;15:39–46.
- [51] Holmqvist C, Larsson EM, Stahlberg F, Laurin S. Contrast-enhanced thoracic 3D-MR angiography in infants and children. *Acta Radiol* 2001;42:50–8.
- [52] Bogaert J, Kuzo R, Dymarkowski S, et al. Follow-up of patients with previous treatment for coarctation of the thoracic aorta: comparison between contrast-enhanced MR angiography and fast spin-echo MR imaging. *Eur Radiol* 2000;10:1847–54.
- [53] Finn JP, Zisk JH, Edelman RR, et al. Central venous occlusion: MR angiography. *Radiology* 1993;187:245–51.
- [54] Hartnell GG, Hughes LA, Finn JP, Longmaid III HE. Magnetic resonance angiography of the central chest veins: a new gold standard? *Chest* 1995;107:1053–7.
- [55] Li W, David V, Kaplan R, Edelman RR. Three-dimensional low dose gadolinium-enhanced peripheral MR venography. *J Magn Reson Imaging* 1998;8:630–3.
- [56] Lebowitz JA, Rofsky NM, Krinsky GA, Weinreb JC. Gadolinium-enhanced body MR venography with subtraction technique. *AJR Am J Roentgenol* 1997;169:755–8.
- [57] Thornton MJ, Ryan R, Varghese JC, et al. A three-dimensional gadolinium-enhanced MR venography technique for imaging central veins. *AJR Am J Roentgenol* 1999;173:999–1003.
- [58] Kroencke TJ, Taupitz M, Arnold R, et al. Three-dimensional gadolinium-enhanced magnetic resonance venography in suspected thrombo-occlusive disease of the central chest veins. *Chest* 2001;120:1570–6.
- [59] Shinde TS, Lee VS, Rofsky NM, et al. Three-dimensional gadolinium-enhanced MR venographic evaluation of patency of central veins in the thorax: initial experience. *Radiology* 1999;213:555–60.
- [60] Goyen M, Barkhausen J, Kuehl H, et al. [Contrast-enhanced 3D MR venography of central thoracic veins: preliminary experience]. *Rofo Fortschr Geb Rontgenstr Neuen Bildgeb Verfahr* 2001;173:356–61.
- [61] Spuentrup E, Buecker A, Stuber M, Gunther RW. MR-venography using high resolution True-FISP. *Rofo Fortschr Geb Rontgenstr Neuen Bildgeb Verfahr* 2001;173:686–90.
- [62] Kauczor HU, Gamroth AH, Tuengerthal SJ, et al. [MR angiography: its use in pulmonary and mediastinal space-occupying lesions]. *Rofo Fortschr Geb Rontgenstr Neuen Bildgeb Verfahr* 1992;157:15–20.
- [63] Gupta A, Frazer CK, Ferguson JM, et al. Acute pulmonary embolism: diagnosis with MR angiography. *Radiology* 1999;210:353–9.
- [64] Kauczor HU, Heussel CP, Thelen M. Update on diagnostic strategies of pulmonary embolism. *Eur Radiol* 1999;9:262–75.
- [65] Meaney JF, Johansson LO, Ahlstrom H, Prince MR. Pulmonary magnetic resonance angiography. *J Magn Reson Imaging* 1999;10:326–38.
- [66] Wielopolski PA, Hicks SG, de Bruin HG, Oudkerk M. Breath-hold three-dimensional lung perfusion imaging and pulmonary angiography after contrast administration. In: Oudkerk M, Edelman RR, editors. *High-power gradient MR-imaging: advances in MRI*. Oxford: Blackwell Science; 1997. p. 71.
- [67] Goyen M, Ruehm SG, Jagenburg A, et al. Pulmonary arteriovenous malformation: characterization with time-resolved ultra-fast 3D MR angiography. *J Magn Reson Imaging* 2001;13:458–60.
- [68] Schoenberg SO, Knopp MV, Grau A, et al. [Ultrafast MRI phlebography of the lungs]. *Radiologe* 1998;38:597–605.